

RECENT RESULTS FROM NA49

C. BLUME FOR THE NA49 COLLABORATION

*Institut für Kernphysik, J.W. Goethe Universität Frankfurt,
Max-von-Laue Str. 1, 60438 Frankfurt am Main, Germany*



New results of the NA49 collaboration on strange particle production are presented. Rapidity and transverse mass spectra as well as total multiplicities are discussed. The study of their evolution from AGS over SPS to the highest RHIC energy reveals a couple of interesting features. These include a sudden change in the energy dependence of the m_t -spectra and of the yields of strange hadrons around 30 AGeV. Also, fluctuations of the $(K^+ + K^-)/(\pi^+ + \pi^-)$ ratio and the $(p + \bar{p})/(\pi^+ + \pi^-)$ ratio, as well as the v_2 of Λ in Pb+Pb collisions at 158 AGeV are discussed.

1 Introduction

In the recent years the NA49 experiment has collected data on Pb+Pb collisions at beam energies between 20 to 158 AGeV with the objective to cover the critical region of energy densities where the expected phase transition to a deconfined phase might occur in the early stage of the reactions. NA49 is a fixed target experiment at the CERN SPS. Details on the experimental setup can be found in¹.

2 Rapidity and transverse mass spectra

An increase of the RMS-widths of the rapidity spectra with beam energy can be observed which for the pions exhibits to a good approximation a linear dependence on the beam rapidity in the center-of-mass system y_{beam} over the whole energy range covered by the AGS and SPS (see Fig. 1). Between 20 AGeV and 158 AGeV this is also true for the other particle types having a Gaussian-like distribution, with a clear hierarchy in the widths: $\sigma(\pi^-) > \sigma(K^+) > \sigma(K^-) \approx \sigma(\phi) > \sigma(\bar{\Lambda})$. However, this seems to break down at lower energies, where the widths of the kaons apparently approach the ones of the pions.

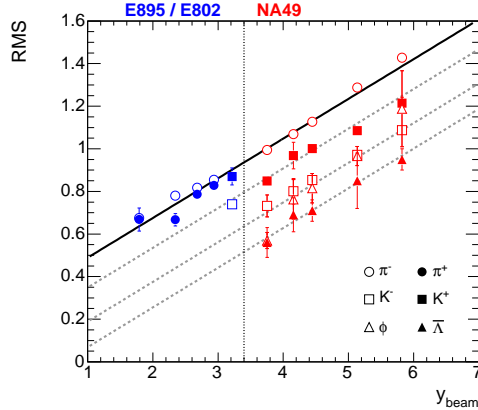


Figure 1: The RMS values of the rapidity distributions of π^\pm , K^\pm , ϕ , and $\bar{\Lambda}$ in central Pb+Pb (Au+Au) collisions as a function of y_{beam} . AGS data are taken from ^{2,3}. The solid line is a linear fit to the pion data. The dashed lines have the same slope, but shifted to match the other particle species.

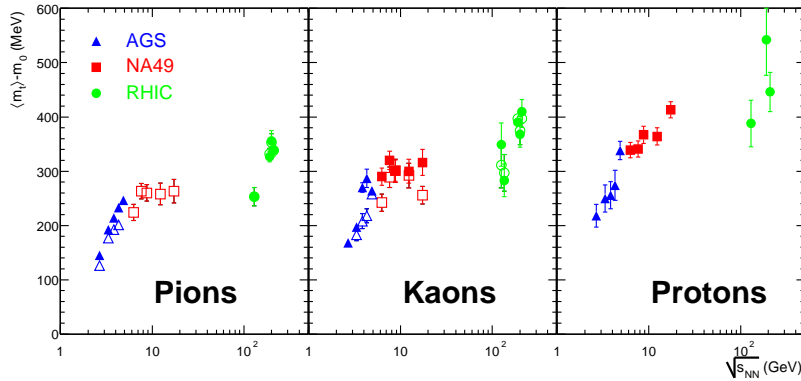


Figure 2: The energy dependence of $\langle m_t \rangle - m_0$ for pions, kaons, and protons at mid-rapidity for 5 (10%) most central Pb+Pb/Au+Au reactions. Open symbols represent negatively charged particles.

The increase with energy of the inverse slope parameter T of the kaon m_t -spectra, as derived from an exponential fit, exhibits a sharp change to a plateau around 30 AGeV^4 . Since the kaon m_t -spectra – in contrast to the ones of the lighter pions or the heavier protons – have to a good approximation an exponential shape, the inverse slope parameter provides in this case a good characterization of the spectra. For other particle species, however, the local slope of the spectra depends on m_t . Instead, the first moment of the m_t -spectra can be used to study their energy dependence. The dependence of $\langle m_t \rangle - m_0$ on the center of mass energy $\sqrt{s_{\text{NN}}}$ is summarized in Fig. 2. The change of the energy dependence around a beam energy of $20 - 30 \text{ AGeV}$ is clearly visible for pions and kaons. While $\langle m_t \rangle - m_0$ rises steeply in the AGS energy range, the rise is much weaker from the low SPS energies on. To a lesser extent this change is also seen for protons.

3 Particle yields

In Fig. 3 the energy dependence of the total multiplicities for a variety of strange hadrons, normalized to the pion yield, is summarized and compared to model predictions. Generally, it can be stated that the string hadronic models UrQMD and HSD ^{5,6} do not provide a good description of the data points. Especially the Ξ and Ω production is substantially underestimated and the maximum in the K^+/π^+ ratio is not reproduced. The statistical hadron gas models ^{7,8},

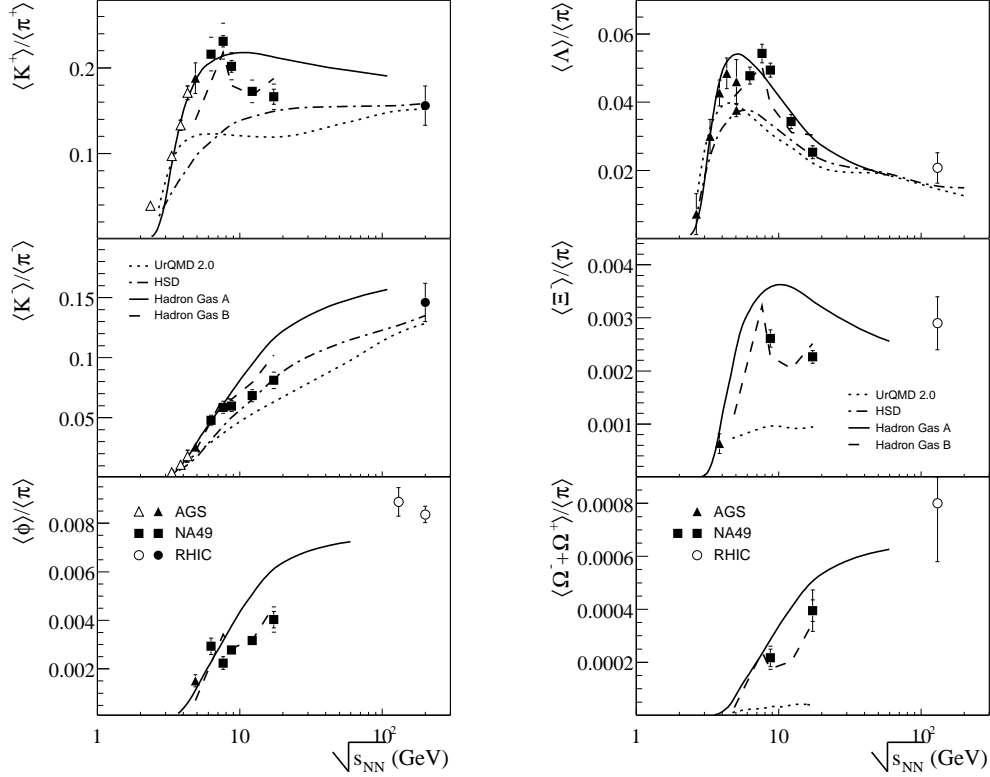


Figure 3: The energy dependence of the 4π -yields of strange hadrons, normalized to the pion yields, in central Pb+Pb/Au+Au collisions. The data are compared to string hadronic models^{5,6} (UrQMD 2.0: dotted lines, HSD: dashed-dotted lines) and statistical hadron gas models^{7,8} (with strangeness under-saturation: dashed line, assuming full equilibrium: solid line).

on the other hand, provide a better overall description of the measurements. However, the introduction of an energy dependent strangeness under-saturation factor γ_S is needed⁸, in order to capture the structures in the energy dependence of most particle species (K^+ , K^- , ϕ , Ξ). The rapid changed of the hadron production properties observed at low SPS energies may be related to the onset of deconfinement⁴.

4 Fluctuations

A study of the energy dependence of event-by-event fluctuations is given in Fig. 4. It shows the fluctuation signal of the $(K^+ + K^-)/(\pi^+ + \pi^-)$ ratio and the $(p + \bar{p})/(\pi^+ + \pi^-)$ ratio. The dynamical fluctuations are derived as the difference to a mixed events reference sample ($\sigma_{\text{dyn.}} = \text{sign}(\sigma_{\text{data}}^2 - \sigma_{\text{mix}}^2) \sqrt{(|\sigma_{\text{data}}^2 - \sigma_{\text{mix}}^2|)}$). As shown in the left panel of Fig. 4, the K/π fluctuations are positive and decrease with beam energy. The p/π fluctuations, on the other hand, are negative – indicating a correlation present in the real data – and increase with beam energies. While the trend of the K/π fluctuations is not reproduced by UrQMD⁵, it provides a good description of the energy dependence of the p/π fluctuations. This might indicate that the negative value of the fluctuations in this ratio is due to resonance decays.

5 Λ -Flow

Figure 5 shows the first results on elliptic flow of Λ from NA49. The comparison to the proton v_2 reveals a clear difference in the p_t -dependence. Also, the increase of v_2 with p_t is much more

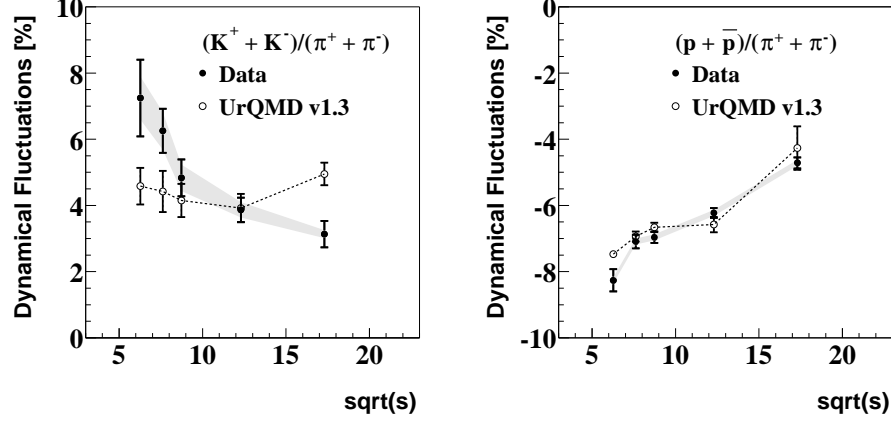


Figure 4: Energy dependence of the event-by-event fluctuation signal of the $(K^+ + K^-)/(\pi^+ + \pi^-)$ ratio (left hand side) and the $(p + \bar{p})/(\pi^+ + \pi^-)$ ratio (right hand side) as measured by NA49⁹. The systematic errors of the measurements are shown as gray bands.

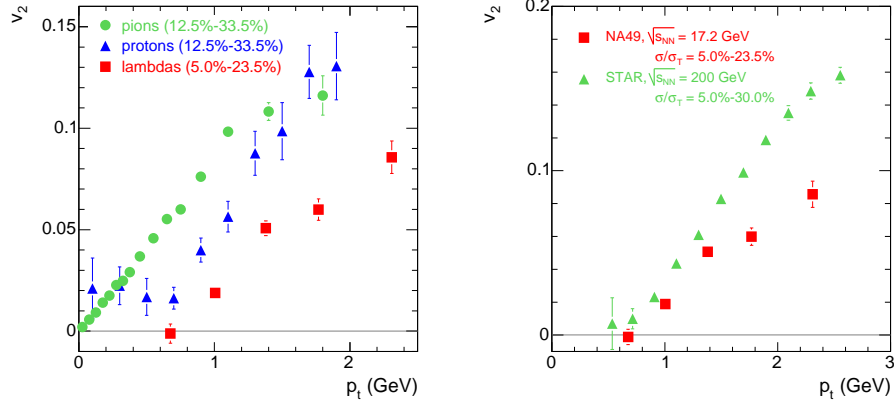


Figure 5: Left: The v_2 of charged pions, protons, and Λ as a function of p_t in semi-central Pb+Pb collisions at $\sqrt{s_{NN}} = 17.2$ GeV. Please note the difference in centrality selection. Right: The v_2 for Λ measured at $\sqrt{s_{NN}} = 17.2$ GeV and $\sqrt{s_{NN}} = 200$ GeV¹⁰.

pronounced at higher $\sqrt{s_{NN}}$ (see right hand side of Fig. 5).

References

1. S.V. Afanasiev et al. (NA49 collaboration), Nucl. Instrum. Meth. **A 430** (1999), 210.
2. J.L. Klay et al. (E895 Collaboration), Phys. Rev. **C 68** (2003), 054905.
3. L. Ahle et al. (E802 collaboration), Phys. Rev **C 57** (1998), 466.
4. M. Gaździcki (for the NA49 collaboration), J. Phys. **G 30** (2004), S701.
5. M. Bleicher et al., J. Phys. **G 25** (1999), 1859.
6. E.L. Bratkovskaya et al., Phys. Rev. **C 69** (2004), 054907.
7. P. Braun-Munzinger, J. Cleymans, H. Oeschler, and K. Redlich, Nucl. Phys. **A 697** (2002), 902.
8. F. Becattini, M. Gaździcki, A. Keränen, J. Manninen, and R. Stock, Phys. Rev. **C 69** (2004), 024905.
9. C. Roland (for the NA49 collaboration), J. Phys. **G 30** (2004), S1381.
10. J. Adams et al. (STAR collaboration), Phys. Rev. Lett. **92** (2004), 052302.